

Relationship between the spatial position of the seed and growth mode for single-crystal diamond grown with an enclosed-type holder

Wen-Liang Xie(谢文良), Xian-Yi Lv(吕宪义), Qi-Liang Wang(王启亮),Liu-An Li(李柳暗), and Guang-Tian Zou(邹广田)

Citation: Chin. Phys. B, 2022, 31 (**10**): 108106. DOI: 10.1088/1674-1056/ac7e35
Journal homepage: http://cpb.iphy.ac.cn; http://iopscience.iop.org/cpb

What follows is a list of articles you may be interested in

Determination of band alignment between GaO_x and boron doped diamond for a selective-area-doped termination structure

Qi-Liang Wang(王启亮), Shi-Yang Fu(付诗洋), Si-Han He(何思翰), Hai-Bo Zhang(张海波),Shao-Heng Cheng(成绍恒), Liu-An Li(李柳暗), and Hong-Dong Li(李红东)

Chin. Phys. B, 2022, 31 (**8**): 088104. DOI: 10.1088/1674-1056/ac464e

Synergistic influences of titanium, boron, and oxygen on large-size single-crystal diamond growth at high pressure and high temperature

Guang-Tong Zhou(周广通), Yu-Hu Mu(穆玉虎), Yuan-Wen Song(宋元文), Zhuang-Fei Zhang(张壮飞), Yue-Wen Zhang(张跃文), Wei-Xia Shen(沈维霞), Qian-Qian Wang(王倩倩), Biao Wan(万彪), Chao Fang(房超), Liang-Chao Chen(陈良超), Ya-Dong Li(李亚东), and Xiao-Peng Jia(贾晓鹏)

Chin. Phys. B, 2022, 31 (**6**): 068103. DOI: 10.1088/1674-1056/ac4650

Multiple enlarged growth of single crystal diamond by MPCVD with PCD-rimless top surface

Ze-Yang Ren(任泽阳), Jun Liu(刘俊), Kai Su(苏凯), Jin-Feng Zhang(张金风), Jin-Cheng Zhang(张进成), Sheng-Rui Xu(许晟瑞), Yue Hao(郝跃)

Chin. Phys. B, 2019, 28 (**12**): 128103. DOI: 10.1088/1674-1056/ab53cd

Preparation of few-layer graphene-capped boron nanowires and their field emission properties

Yong-Xin Zhang(张永欣), Fei Liu(刘飞), Cheng-Min Shen(申承民), Tian-Zhong Yang(杨天中), Jun Li(李军), Shao-Zhi Deng(邓少芝), Ning-Sheng Xu(许宁生), Hong-Jun Gao(高鸿钧)

Chin. Phys. B, 2016, 25 (**7**): 078101. DOI: 10.1088/1674-1056/25/7/078101

SPECIAL TOPIC — Celebrating the 70th Anniversary of the Physics of Jilin University

Relationship between the spatial position of the seed and growth mode for single-crystal diamond grown with an enclosed-type holder

Wen-Liang Xie(谢文良)[1,2], Xian-Yi Lv(吕宪义)[1,2], Qi-Liang Wang(王启亮)[1,2], Liu-An Li(李柳暗)[1,2,†], and Guang-Tian Zou(邹广田)[1,2,‡]

[1] *State Key Laboratory of Superhard Materials, Jilin University, Changchun* 130012, *China*
[2] *Shenzhen Research Institute, Jilin University, Shenzhen* 518057, *China*

(Received 3 April 2022; revised manuscript received 17 June 2022; accepted manuscript online 5 July 2022)

The relationship between the spatial position of the diamond seed and growth mode is investigated with an enclosed-type holder for single-crystal diamond growth using the microwave plasma chemical vapor deposition epitaxial method. The results demonstrate that there are three main regions by varying the spatial position of the seed. Due to the plasma concentration occurring at the seed edge, a larger depth is beneficial to transfer the plasma to the holder surface and suppress the polycrystalline diamond rim around the seed edge. However, the plasma density at the edge decreases drastically when the depth is too large, resulting in the growth of a vicinal grain plane and the reduction of surface area. By adopting an appropriate spatial location, the size of single-crystal diamond can be increased from 7 mm × 7 mm × 0.35 mm to 8.6 mm × 8.6 mm × 2.8 mm without the polycrystalline diamond rim.

Keywords: MPCVD, single-crystal diamond growth, enclosed-type holder, growth mode modulation

PACS: 81.05.ug, 77.84.Bw, 73.40.Kp, 82.80.Pv **DOI:** 10.1088/1674-1056/ac7e35

1. Introduction

Diamond is a promising material with outstanding characteristics, such as excellent thermal conductivity, good light transmittance, high electron and hole mobility, and a wide bandgap.[1–3] Diamond has broad application prospects and is expected to be used in many fields in the future.[4,5] However, the size of high-temperature–high-pressure single-crystal diamond (SCD) that can be industrially mass produced is generally smaller than 15 mm, which does not meet the requirements of diamond applications in many fields.[6] Therefore, various methods have been proposed to increase the size of SCD.[7–12] Among these methods, microwave plasma chemical vapor deposition (MPCVD) is the most promising method due to the high purity and high plasma density. By using an MPCVD system, SCD with a thickness of 10 mm has been obtained through repeated three-dimensional growth. Furthermore, SCD with a large area of 40 mm × 60 mm has been achieved by mosaic growth.[11,12]

Although great progress has been made up to now, a polycrystalline diamond rim usually appears at the edges of the diamond seed.[13] This polycrystalline diamond rim significantly affects the growth of SCD, not only preventing lateral epitaxial growth, but also reducing the effective area of the top surface due to the inward growth of the polycrystalline diamond.[14] Generally, the concentration of microwave plasma at the sharp edges of the seed is regarded as the main cause of the formation of the polycrystalline diamond rim. To solve this problem, an enclosed-type holder is fabricated to reduce plasma attraction at the edges of SCD, which helps to suppress the generation of the polycrystalline diamond rim.[15] However, the enclosed-type holder does not function as expected if the seed is improperly placed. As a result, the seed growth may still be affected by the plasma concentration at the edges, resulting in the appearance of a polycrystalline diamond rim.[13,16,17]

In this study, the relationship between the spatial location and growth mode of diamond seeds in an enclosed-type holder is explored. The preferred growth region is obtained to achieve relatively stable and repeatable growth. Based on the results, the size of SCD is increased from 7 mm × 7 mm × 0.35 mm to 8.6 mm × 8.6 mm × 2.8 mm without the polycrystalline diamond rim.

2. Experiment

Diamond was grown in a 2.45 GHz, 5 kW MPCVD reactor (WSPS-2450-5K-CEWG, NIUMANHERUI, Chengdu), with the growth temperature measured by a stationary one-color pyrometer through a quartz viewing port. The total thickness of the enclosed-type holder was approximately 5 mm, and the dimensions of the central square hole were 10 mm × 10 mm. The SCD seeds were commercial (100)-

†Corresponding author. E-mail: liliuan@jlu.edu.cn
‡Corresponding author. E-mail: gtzou@jlu.edu.cn

© 2022 Chinese Physical Society and IOP Publishing Ltd

oriented chemical vapor deposition grown samples with different dimensions to adjust the spatial position.

Prior to growth, each diamond seed was ultrasonically cleaned with acetone and alcohol. Then, the seed was *in situ* etched in the MPCVD chamber for 10 min with 3 sccm O_2 and 400 sccm H_4 at approximately 900 °C. High-purity methane (CH_4), oxygen (O_2), and hydrogen (H_2) were used as reaction gases with flow rates of 20 sccm, 3 sccm, and 400 sccm, respectively. During the growth process, the temperature was automatically controlled at approximately 950 °C, the pressure was controlled at approximately 260 Torr, and the microwave power was controlled at 2800 W–3400 W. The temperature was kept stable by simultaneously adjusting the microwave power and pressure.

The average growth rates were calculated by dividing the total incremental thickness at the center surface (measured by a micrometer) by the deposition time. The diamond morphology surface was characterized by an optical microscope, and the crystalline quality of the prepared samples was observed by Raman spectroscopy (Horiba-JY T64000).

3. Results and discussion

Figure 1(a) presents an optical image of the plasma concentration at the edge of the enclosed-type holder, while Fig. 1(b) presents a schematic diagram of the structure of the enclosed-type holder with a SCD seed. As displayed in Fig. 1(b), two parameters — width (W; interval between the seed edge and holder edge) and depth (D; interval between the seed top surface and holder top surface) — are defined to represent the spatial positional relationship between the seed and holder. Prior to growth, all dimensions of the seeds are measured and recorded (detailed information can be found in Table S1). The depth is usually adjusted by inserting Mo sheets with different thicknesses beneath the diamond seeds. The width is determined by the size discrepancy between the seed and the hole.

The effect of the spatial position of the seeds on the growth mode under identical growth conditions is summarized in Fig. 2(a). By combining the microscope images of the typical surface topography, three different growth modes are identified: polycrystalline rim (Fig. 2(b)), single-crystal (Fig. 2(c)), and shrinking (Fig. 2(d)) modes. In Fig. 2(a), the red, green, and blue dots represent the polycrystalline rim, single-crystal, and shrinking regions, respectively. It can be seen from Fig. 2(a) that a greater depth is required for single-crystal growth when a larger width is adopted.

Generally, both plasma density and temperature are correlated with diamond growth in an MPCVD system. Li *et al.* simulated the effect of seed thickness on the electric field intensity and electron density distribution on substrate surfaces with an open holder.[18] They find that both the electric field and electron density are strengthened at the edges and corners, resulting in a higher temperature at the edges. Mokuno *et al.* observed a convex surface for a sample with a relatively large depth in an enclosed type holder, indicating that diamond do not grow at the four corners.[19] A possible reason is that the corners are close to the surrounding Mo holder with lower temperature, resulting in the suppression of nucleation and a decrease in the growth rate. The above discussion suggests that the holder can not only change the plasma density but also affect the heat dissipation of the seed. This assumption is confirmed by Wu *et al.*, who demonstrates that the growth rates of samples decrease significantly when the recess depth increase.[20]

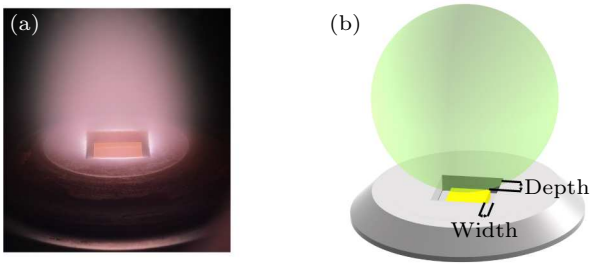


Fig. 1. (a) Optical image of the plasma concentration at the edge of the enclosed-type holder in the experiment. (b) Schematic structure of the enclosed-type holder with a seed.

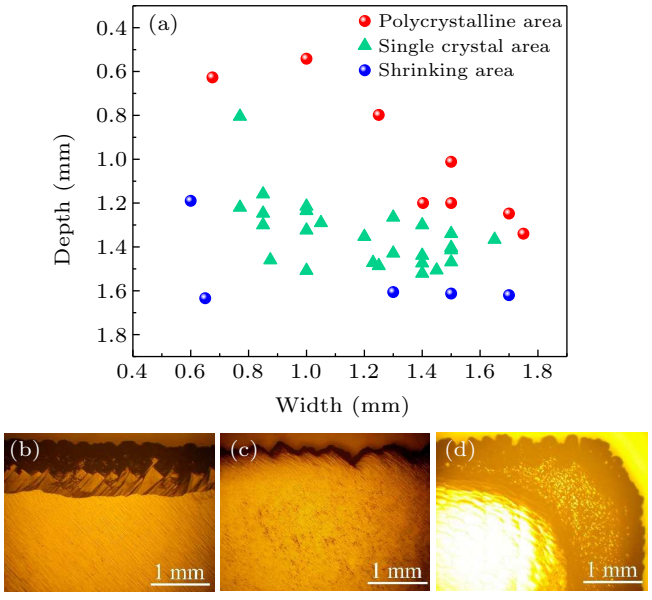


Fig. 2. (a) Relationship between the growth mode and spatial position of the seed. (b)–(d) Optical images corresponding to the typical morphologies of (b) polycrystalline (D = 1.01 mm, W = 1.5 mm), (c) single-crystal (D = 1.35 mm, W = 1.2 mm), and (d) shrinking surface modes (D = 1.34 mm, W = 1.5 mm).

When no holder is used or the width is relatively large, the plasma concentrates at the edge of the diamond seed. As a result, a higher temperature and higher growth rate occurs at the edge, resulting in the appearance of a polycrystalline diamond rim (band in Figs. 3(a)–3(c)). Therefore, a greater depth can help to shift the plasma concentration to the edge of the enclosed-type holder. Simultaneously, the top surface

of the diamond sample is entirely covered by plasma, resulting in SCD growth (Figs. 3(d)–3(f)). However, only the center of the sample surface is covered by plasma when the depth is larger than a critical value. The distance between the diamond edge and plasma ball increases, which reduces the precursors and radical concentration on the diamond surface (Fig. 1(a)). In addition, the surrounding Mo holder improves the heat dissipation of the sample. The temperature at the edge is approximately 10 °C lower than that at the center in the experiments. The growth rate of the edge is thus much lower than that of the center region, resulting in the enhancing growth of the vicinal crystalline plane and shrinking surface area (Fig. 3(g)).

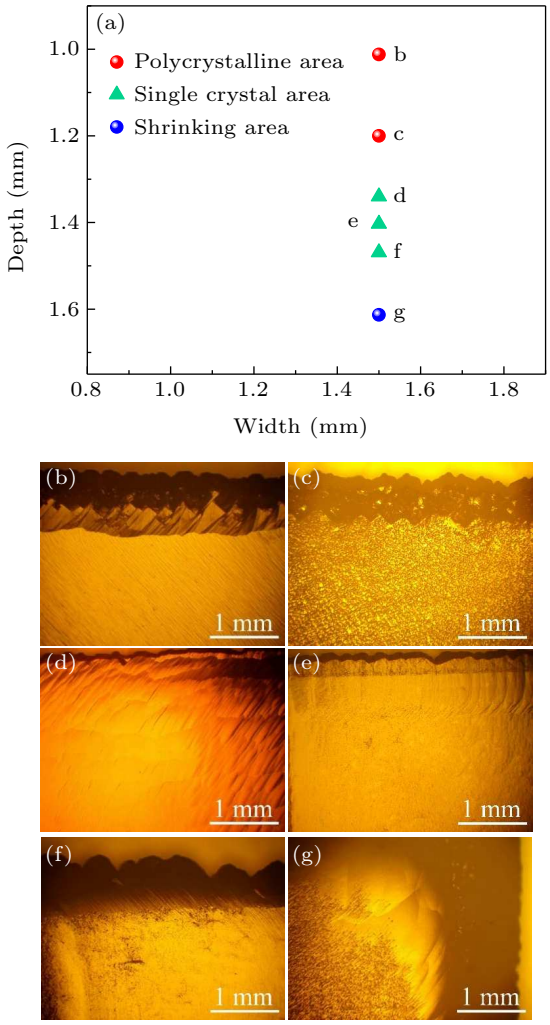


Fig. 3. (a) Variation in growth mode at different sample depths with the same width. (b)–(g) Optical microscope images of the surface morphology of samples labeled b–g in (a).

Figures 4(a) and 4(b) illustrate the growth rates of the samples within the single-crystal region versus depth and width, respectively. It can be seen that although the growth rates of the samples at different spatial positions fluctuates, they are still comparable to each other and fall within a relatively small range. Therefore, the variation in spatial positions in the single-crystal region has no obvious effect on the plasma (growth) conditions. The slight difference in the growth rate is ascribed to the difference in the chamber pressure during the automatic temperature adjustment process. Based on the above discussion, the surface morphology and growth rate of samples in the single-crystal region are stable and repeatable under the present growth conditions, which provides a basis for increasing the three-dimensional size of diamond.

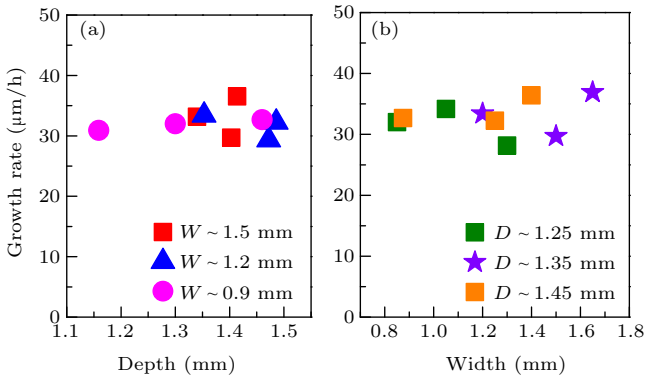


Fig. 4. Growth rates of samples within the single-crystal region versus (a) depth (D) and (b) width (W). The variation in the growth rate is small for all positions.

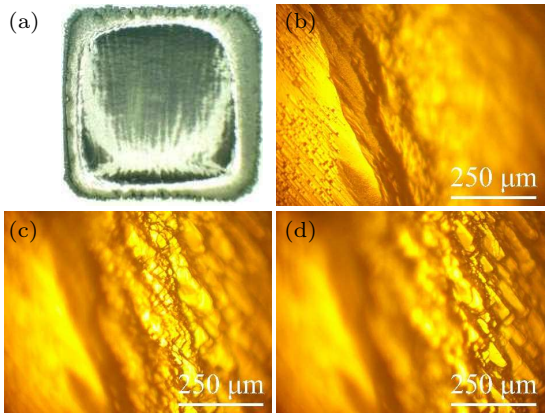


Fig. 5. (a) Bird's eye view of single-crystal diamond after growth (D = 1.6 mm and W = 1.5 mm). (b)–(d) Zoomed-in optical microscope images near the edge at different focal depths. A change in focal depth implies a change in height.

The typical surface morphology of the sample after growth in the shrinking region is presented in Fig. 5. Figure 5(a) clearly indicates that the effective area of the top (001) surface shrinks after growth. Figures 5(b)–5(d) display the zoomed-in top surface near the edge for the samples at different focal depths. The results demonstrate that the thickness of the diamond increases from the edge to the center in many small steps. This phenomenon can be ascribed to the following two main causes. First, the edge of the seed is far away from the plasma at a relatively large depth, and the plasma is attracted by the holder. Second, the polycrystalline diamond film grows on the holder surface during the growth process also increases the plasma attraction. The plasma density and growth rate of the SCD near the edge are relatively small, resulting in the formation of the discontinuous small step-like morphology. With increasing growth time, the vicinal grain

plane gradually appears and expands from the edges of the inside, forming the morphology displayed in Fig. 5.

To evaluate the crystalline quality of the SCD grown with different spatial positions, the Raman spectra of diamond are measured at the center of the top surface (Fig. 6). Three samples with the same width but different depths are selected for evaluation. Both sample 1 (S1; $D = 1.16$ mm, $W = 0.85$ mm) and sample 2 (S2; $D = 1.51$ mm, $W = 1.0$ mm) are in the single-crystal region. Sample 3 (S3; $D = 0.54$ mm, $W = 1.0$ mm) is in the polycrystalline region. The full width at half maximum of samples 1–3 are 2.98 cm^{-1}, 2.95 cm^{-1}, and 2.95 cm^{-1}, and the Raman peak positions are 1331.53 cm^{-1}, 1330.93 cm^{-1}, and 1331.53 cm^{-1}, respectively. Therefore, the crystalline quality at the center is not obviously degraded by the spatial positions even with the existence of the polycrystalline diamond rim. This can be attributed to the fact that the variation in the spatial positions of the seeds mainly affects the edge of the seed while having no obvious effect on the surface region, which is covered by plasma.

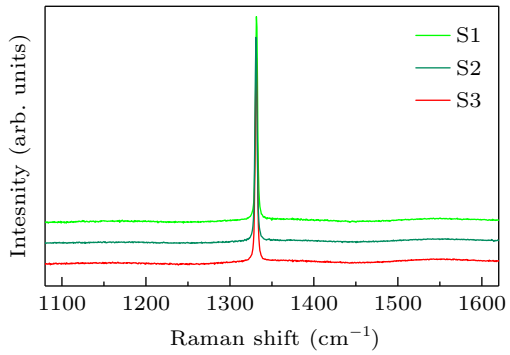


Fig. 6. Raman spectra of three samples grown in the single-crystal and polycrystalline regions. The crystalline quality at the center is not obviously degraded by the spatial positions.

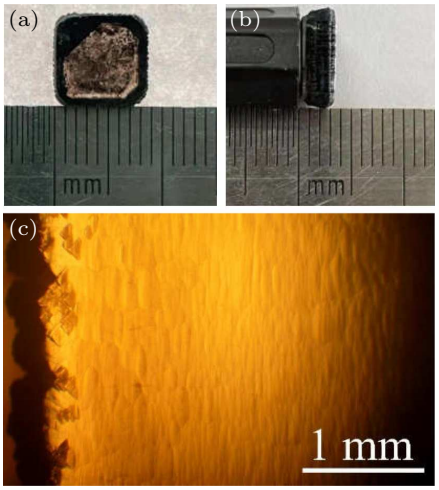


Fig. 7. (a) Bird's-eye view, (b) cross-sectional view, and (c) optical microscope image of single-crystal diamond surface morphology obtained by repeating growth for 110 h. The initial size is approximately 7 mm × 7 mm × 0.35 mm.

Finally, by choosing the conditions of the single-crystal region in Fig. 2, a SCD with a size of 8.6 mm × 8.6 mm × 2.8 mm is obtained by repeating the growth for 110 h (Fig. 7). Observed from the bird's eye view (Fig. 7(a)) and cross-sectional view images (Fig. 7(b)), the seed is enlarged in both the vertical and lateral directions due to the suppression of the polycrystalline diamond rim. There is some graphite and/or non-diamond carbon on the backside of the SCD, which hinders the transmittance of light and reduces the transparency. The surface morphology in the microscope image of the sample (Fig. 7(c)) is similar to that presented in Fig. 3. The surface is smooth and flat, and there is no polycrystalline diamond at the edges, which demonstrates the stability of the growth conditions. The thick epitaxial layer can be saw into several thin seeds for the mosaic growth of inch-class SCD wafers in the future.

4. Conclusion and perspectives

In conclusion, an enclosed-type holder is adopted for SCD growth using the MPCVD epitaxial method, and the corresponding relationship between the spatial position of the seed and the growth mode is evaluated. The surface morphology indicates that the growth behavior can be divided into three main regions: the polycrystalline rim region, single-crystal region, and shrinking region. For samples with a relatively large width, the plasma concentrates at the edge of the diamond seed, which causes the appearance of the polycrystalline diamond rim. A larger depth is thus beneficial to shift the plasma concentration to the edge of the enclosed-type holder and to ensure SCD growth. However, the growth rate is too low when the depth is larger than a critical value, resulting in the increases growth of the vicinal crystalline plane and a shrinking surface area. This variation in the growth modes is the balance between the holder and the ellipsoid shape of plasma, which is confirmed by the fact that the growth rate and crystalline quality are nearly identical for different samples. Finally, by adopting an appropriate spatial location, the SCD size could be increased from 7 mm × 7 mm × 0.35 mm to 8.6 mm × 8.6 mm × 2.8 mm without the polycrystalline diamond rim. These results provide a basis for further increasing the area of the diamond substrate or as a large-size diamond seed.

Acknowledgment

Project supported by the Key-Area Research and Development Program of Guangdong Province, China (Grant No. 2020B0101690001).

References

[1] Ukhina A V, Dudina D V, Esikov M A, Samoshkin D A, Stankus S V, Skovorodin I N, Galashov E N and Bokhonov B B 2020 *Surf. Coat. Tech.* **401** 126272

[2] Arnault J C, Saada S and Ralchenko V 2021 *Phys. Status. Solidi-R* **16** 2100354
[3] Sanders N and Kioupakis E 2021 *Appl. Phys. Lett.* **119** 062101
[4] Gabrysch M, Majdi S, Twitchen D J and Isberg J 2011 *J. Appl. Phys.* **109** 063719
[5] Donato N, Rouger N, Pernot J, Longobardi G and Udrea F 2019 *J. Phys. D. Appl. Phys.* **53** 093001
[6] Shu G, Dai B, Bolshakov A, Wang W, Wang Y, Liu K, Zhao J, Han J and Zhu J 2021 *Function Diamond* **1** 47
[7] Yamada H, Chayahara A, Mokuno Y, Umezawa H, Shikata S I and Fujimori N 2010 *Appl. Phys. Express.* **3** 051301
[8] Yamada H, Chayahara A, Mokuno Y, Tsubouchi N and Shikata S I 2013 *Diam. Relat. Mater.* **33** 27
[9] Yamada H, Chayahara A, Umezawa H, Tsubouchi N, Mokuno Y and Shikata S 2012 *Diam. Relat. Mater.* **24** 29
[10] Yamada H, Chayahara A, Mokuno Y, Tsubouchi N, Shikata S I and Fujimori N 2011 *Diam. Relat. Mater.* **20** 616
[11] Shu G, Dai B, Ralchenko V G, Khomich A A, Ashkinazi E E, Bolshakov A P, Bokova-Sirosh S N, Liu K, Zhao J, Han J and Zhu J 2017 *J. Cryst. Growth.* **463** 19
[12] Yamada H, Chayahara A, Mokuno Y, Kato Y and Shikata S 2014 *Appl. Phys. Lett.* **104** 102110
[13] Widmann C J, Müller-Sebert W, Lang N and Nebel C E 2016 *Diam. Relat. Mater.* **64** 1
[14] Nad S, Charris A and Asmussen J 2016 *Appl. Phys. Lett.* **109** 162103
[15] Mokuno Y, Chayahara A, Soda Y, Horino Y and Fujimori N 2005 *Diam. Relat. Mater.* **14** 1743
[16] Wu G, Chen M H and Liao J 2016 *Diam. Relat. Mater.* **65** 144
[17] Cao W, Ma Z, Zhao H, Gao D and Fu Q 2022 *CrystEngComm* **24** 1010
[18] Li Y, Liu X, Shu G, Liu K, Zhao J, Zhang S, Yang L, Dai B, Zhu J and Han J 2020 *Diam. Relat. Mater.* **101** 107574
[19] Mokuno Y, Chayahara A, Soda Y, Horino Y and Fujimori N 2005 *Diam. Relat. Mater.* **14** 1743
[20] Wu G, Chen M and Liao J 2016 *Diam. Relat. Mater.* **65** 144